Revised Version

DESY 98-158
CERN-TH/98-368
DTP/98/88

DTP/98/88
CERN-TH/98-368
DESY 98-158
hep-ph/9810290
October 1998

hep-ph/9810290 v3 19 Jan 1999

SUSY Particle Production at the Tevatron*

W. Beenakker[1†], M. Krämer[2], T. Plehn[3‡], and M. Spira[4§]

[1] *Department of Physics, University of Durham, Durham DH1 3LE, U.K.*
[2] *Theory Division, CERN, CH-1211 Geneva 23, Switzerland*
[3] *Dept. of Physics, University of Wisconsin, Madison, USA*
[4] *II. Institut für Theoretische Physik¶, Universität Hamburg, Germany*

Abstract

The calculation of the next-to-leading order SUSY-QCD corrections to the production of squarks, gluinos and gauginos at the Tevatron is reviewed. The NLO corrections stabilize the theoretical predictions of the various production cross sections significantly and lead to sizeable enhancements of the most relevant cross sections for scales near the average mass of the produced massive particles. We discuss the phenomenological consequences of the results on present and future experimental analyses.

*Contribution to the Workshop *Physics at Run II – Supersymmetry/Higgs*, 1998, Fermilab, USA.

†Supported by a PPARC Research Fellowship

‡Supported in part by DOE grant DE-FG02-95ER-40896 and in part by the University of Wisconsin Research Committee with funds granted by the Wisconsin Alumni Research Foundation

§Heisenberg Fellow

¶Supported by Bundesministerium für Bildung und Forschung (BMBF), Bonn, Germany, under Contract 05 7 HH 92P (5), and by EU Program *Human Capital and Mobility* through Network *Physics at High Energy Colliders* under Contract CHRX–CT93–0357 (DG12 COMA).

1 Introduction

The search for supersymmetric particles is among the most important endeavors of present and future high energy physics. At the upgraded $p\bar{p}$ collider Tevatron, the searches for squarks and gluinos, as well as for the weakly interacting charginos and neutralinos, will cover a wide range of the MSSM parameter space [1].

The cross sections for the production of SUSY particles in hadron collisions have been calculated at the Born level already quite some time ago [2]. Only recently have the theoretical predictions been improved by calculations of the next-to-leading order SUSY-QCD corrections [3–5]. The higher-order corrections in general increase the production cross section compared to the predictions at the Born level and thereby improve experimental mass bounds and exclusion limits. Moreover, by reducing the dependence of the cross section on spurious parameters, *i.e.* the renormalization and factorization scales, the cross sections in NLO are under much better theoretical control than the leading-order estimates.

The paper is organized as follows. In Section 2 we shall review the calculation of the next-to-leading order SUSY-QCD corrections [3–5], by using the case of $\tilde{q}\bar{\tilde{q}}$ production as an example. The NLO results for the production of squarks and gluinos are presented in Section 3. We first focus on the scalar partners of the five light quark flavors, which are assumed to be mass degenerate. The discussion of final-state stop particles, with potentially large mass splitting and mixing effects, is presented in Section 4. In Section 5 we discuss the NLO cross sections for the production of charginos and neutralinos. We conclude the paper with a summary of the relevant MSSM particle production cross sections at the upgraded Tevatron, including next-to-leading order SUSY-QCD corrections.[1]

2 SUSY-QCD corrections

The evaluation of the SUSY-QCD corrections consists of two pieces, the virtual corrections, generated by virtual particle exchanges, and the real corrections, which originate from real-gluon radiation as well as from processes with an additional massless (anti)quark in the final state.

[1] The MSSM Higgs sector will not be discussed here, see instead Ref.[6].

2.1 Virtual corrections

The one-loop virtual corrections, *i.e.* the interference of the Born matrix element with the one-loop amplitudes, are built up by gluon, gluino, quark and squark exchange contributions (see Fig. 1a). We have adopted the fermion flow prescription [7] for the calculation of matrix elements including Majorana particles. The evaluation of the one-loop contributions has been performed in dimensional regularization, leading to the extraction of ultraviolet, infrared and collinear singularities as poles in $\epsilon = (4-n)/2$. For the chiral γ_5 coupling we have used the naive scheme, which is well justified in the present analysis at the one-loop level.[2] After summing all virtual corrections no quadratic divergences are left over, in accordance with the general property of supersymmetric theories. The renormalization of the ultraviolet divergences has been performed by identifying the squark and gluino masses with their pole masses, and defining the strong coupling in the $\overline{\rm MS}$ scheme including five light flavors in the corresponding β function. The massive particles, *i.e.* squarks, gluinos and top quarks, have been decoupled by subtracting their contribution at vanishing momentum transfer [8]. In dimensional regularization, there is a mismatch between the gluonic degrees of freedom (d.o.f. $= n-2$) and those of the gluino (d.o.f. $= 2$), so that SUSY is explicitly broken. In order to restore SUSY in the physical observables in the massless limit, an additional finite counter-term is required for the renormalization of the novel $\tilde{q}\tilde{g}\bar{q}$ vertex. These counter-terms have been shown to render dimensional regularization consistent with supersymmetry [9].

2.2 Real corrections

The real corrections are generated by real-gluon radiation off all colored particles and by final states with an additional massless (anti)quark, obtained from interchanging the final state gluon with a light quark in the initial state (see Fig. 1b). The phase-space integration of the final-state particles has been performed in $n = 4-2\epsilon$ dimensions, leading to the extraction of infrared and collinear singularities as poles in ϵ. After evaluating all angular integrals and adding the virtual and real corrections, the infrared singularities cancel. The left-over collinear singularities are universal and are absorbed in the renormalization of the parton densities at next-to-leading order. We have defined the parton densities in the conventional $\overline{\rm MS}$ scheme including five

[2] We have explicitly checked that the results obtained with a consistent γ_5 scheme are identical to those obtained with the naive scheme.

light flavors, *i.e.* the squark, gluino and top quark contributions are not included in the mass factorization. We finally obtain an ultraviolet, infrared and collinear finite partonic cross section.

There is, however, an additional class of physical singularities, which have to be regularized. In the second diagram of Fig. 1b, an intermediate $\tilde{q}\tilde{g}^*$ state is produced, before the (off-shell) gluino splits into a $q\bar{\tilde{q}}$ pair. If the gluino mass is larger than the common squark mass, and the partonic c.m. energy is larger than the sum of the squark and gluino masses, the intermediate gluino can be produced on its mass-shell. Thus the real corrections to $\tilde{q}\bar{\tilde{q}}$ production contain a contribution of $\tilde{q}\tilde{g}$ production. The residue of this part corresponds to $\tilde{q}\tilde{g}$ production with the subsequent gluino decay $\tilde{g} \to \bar{\tilde{q}}q$, which is already contained in the leading order cross section of $\tilde{q}\tilde{g}$ pair production, including all final-state cascade decays. This term has been subtracted in order to derive a well-defined production cross section. Analogous subtractions emerge in all reactions: if the gluino mass is larger than the squark mass, the contributions from $\tilde{g} \to \tilde{q}\bar{q}, \bar{\tilde{q}}q$ have to be subtracted, and in the reverse case the contributions of squark decays into gluinos have to subtracted.

3 Results

In the following, we will present numerical results for SUSY particle production cross sections at the upgraded Tevatron ($\sqrt{s} = 2$ TeV), including SUSY-QCD corrections. The hadronic cross sections are obtained from the partonic cross sections by convolution with the corresponding parton densities. We have adopted the CTEQ4L/M parton densities [10] for the numerical results presented below. The uncertainty due to different parametrizations of the parton densities in NLO is less than ~ 15 %. The average final state particle mass is used as the central value of the renormalization and factorization scales and the top quark mass is set to $m_t = 175$ GeV. The K-factor is defined as $K = \sigma_{NLO}/\sigma_{LO}$, with all quantities ($\alpha_s(\mu_R)$, parton densities, parton cross section) calculated consistently in lowest and in next-to-leading order.

3.1 Production of Squarks and Gluinos

Squarks and gluinos can be produced in different combinations via $p\bar{p} \to \tilde{q}\bar{\tilde{q}}, \tilde{q}\tilde{q}, \tilde{q}\tilde{g}, \tilde{g}\tilde{g}$. We first focus on the five light-flavored squarks, taken to be mass degenerate. At the central renormalization and factorization scale $Q =$

m, where m denotes the average mass of the final-state squarks/gluinos, the SUSY-QCD corrections are large and positive, increasing the total cross sections in general by 10–90% [3]. This is shown in Fig. 2, where the K-factors are presented as a function of the corresponding SUSY particle mass. The inclusion of SUSY-QCD corrections leads to an increase of the lower bounds on the squark and gluino masses by 10–30 GeV with respect to the leading-order analysis.

The residual renormalization/factorization scale dependence in leading and next-to-leading order is presented in Fig. 3. The inclusion of the next-to-leading order corrections reduces the scale dependence by a factor 3–4 relative to the lowest order and reaches a typical level of $\sim 15\%$, when varying the scale from $Q = 2m$ to $Q = m/2$. This may serve as an estimate of the remaining theoretical uncertainty due to uncalculated higher-order terms.

Finally, we have evaluated the QCD-corrected single-particle exclusive transverse-momentum and rapidity distributions for all different processes. As can be inferred from Fig. 4, the modification of the normalized distributions in next-to-leading compared to leading order is less than about 15% for the transverse-momentum distributions and even smaller for the rapidity distributions. It is thus a sufficient approximation to rescale the leading order distributions uniformly by the K-factors of the total cross sections.

3.2 Stop Pair Production

Stop production has to be considered separately since the strong Yukawa coupling between top/stop and Higgs fields gives rise to potentially large mixing effects and mass splitting. At leading-order in the strong coupling constant α_s, only diagonal pairs of stop quarks can be produced in hadronic collisions, $p\bar{p} \to \tilde{t}_1\bar{\tilde{t}}_1/\tilde{t}_2\bar{\tilde{t}}_2$. In contrast to the production of light-flavor squarks, the leading-order t-channel gluino exchange diagram is absent for stop production via $q\bar{q}$ initial states, since top quarks are not included in the parton densities. The leading-order stop cross section is thus in general significantly smaller than the leading order cross section for producing light-flavor squarks, where the threshold behavior is dominated by t-channel gluino exchange. Mixed $\tilde{t}_1\tilde{t}_2$ pair production can safely be neglected since it can proceed only via one-loop α_s or tree level G_F amplitudes and is suppressed by several orders of magnitude [4]. The evaluation of the QCD corrections proceeds along the same lines as in the case of squarks and gluinos.[3] The strong coupling

[3]The results obtained for the case of stop production can also be used to predict the sbottom pair cross section at NLO including mixing and mass splitting.

and the parton densities have been defined in the $\overline{\rm MS}$ scheme with five light flavors contributing to their scale dependences, while the stop masses are renormalized on-shell.

The magnitude of the SUSY-QCD corrections is illustrated by the K-factors at the central scale $Q = m_{\tilde{t}}$ in Fig. 5. In the mass range relevant for the searches at the Tevatron, the SUSY-QCD corrections are positive and reach a level of 30 to 45% if the gg initial state dominates. If, in contrast, the $q\bar{q}$ initial state dominates, the corrections are small. The relatively large mass dependence of the K-factor for stop production at the Tevatron can therefore be attributed to the fact that the gg initial state is important for small $m_{\tilde{t}}$, whereas the $q\bar{q}$ initial state dominates for large $m_{\tilde{t}}$.

In complete analogy to the squark/gluino case, the scale dependence of the stop cross section is strongly reduced, to about 15% at next-to-leading order in the interval $m_{\tilde{t}}/2 < Q < 2m_{\tilde{t}}$. The virtual corrections at the NLO level depend on the stop mixing angle, the squark and gluino masses, and on the mass of the second stop particle. It turns out, however, that these dependences are very weak for canonical SUSY masses and can safely be neglected, as can be inferred from the light-stop production cross section in Fig. 5. On the other hand, internal particles with masses smaller than the external particle mass, e.g. a light stop state propagating in the loops for heavy stop production, will contribute to the cross section. This feature explains the small but noticeable difference between the $\tilde{t}_1$ and $\tilde{t}_2$ K-factors at $m_{\tilde{t}} = 300$ GeV shown in Fig. 5.

The next-to-leading order transverse-momentum and rapidity distributions are presented in Fig. 6. While the shape of the rapidity distribution is almost identical at leading and next-to-leading order, the transverse momentum carried away by hard gluon radiation in higher orders softens the NLO transverse momentum distribution considerably.

3.3 Chargino and Neutralino Production

At leading order, the production cross sections for chargino and neutralino final states depend on several MSSM parameters, *i.e.* M_1, M_2, μ and $\tan\beta$ [2]. The cross sections are sizeable for chargino/neutralino masses below about 100 GeV at the upgraded Tevatron. Due to the strong sensitivity to the MSSM parameters, the extracted bounds on the chargino and neutralino masses depend on the specific region in the MSSM parameter space [1]. The outline of the determination of the QCD corrections is analogous to the previous cases of squarks, gluinos and stops. The resonance contributions

due to $gq \to \tilde{\chi}_i \tilde{q}$ with $\tilde{q} \to q\tilde{\chi}_j$ have to be subtracted in order to avoid double counting of the associated production of electroweak gauginos and strongly interacting squarks. The parton densities have been defined with five light flavors contributing to their scale evolution in the $\overline{\rm MS}$ scheme, while the t-channel squark masses have been renormalized on-shell.[4]

At the average mass scale, the QCD corrections enhance the production cross sections of charginos and neutralinos typically by about 10–35% (see Fig. 7), depending in detail on the final state and the choice of MSSM parameters. The leading order scale dependence is reduced to about 10% at next-to-leading order (see Fig. 7), which implies a significant stabilization of the theoretical prediction for the production cross sections [5].

The individual leading order contributions of the s-channel gauge boson and the t, u-channel squark exchange are presented in Fig. 8. For neutralino pair production the $(t + u)$-channel contributions are by far dominating, while the s-channel and interference terms are suppressed. Since the $\tilde{\chi}^0_{1,2}$ states are predominantly gaugino-like, this reflects the absence of a purely neutral trilinear gauge boson coupling in the Standard Model. Contrary to that the s-channel of $\tilde{\chi}^\pm_1 \tilde{\chi}^0_2$ production is dominant and the $(t + u)$-channel term is suppressed for large squark masses. However, the interference turns out to be sizeable.

4 Conclusions

We have reviewed the status of SUSY particle production at the upgraded Tevatron at next-to-leading order in supersymmetric QCD. A collection of relevant sparticle production cross sections is shown in Fig. 9. The higher-order corrections at the average mass scale of the massive final-state particles significantly increase the production cross section compared to the predictions at the Born level. Experimental mass bounds are therefore shifted upwards. Moreover, the theoretical uncertainties due to variation of renormalization/factorization scales are strongly reduced to a level of typically ~ 15 %, so that the cross sections in next-to-leading order SUSY-QCD are under much better theoretical control than the leading order estimates. The NLO results for total cross sections and differential distributions are available

[4] The next-to-leading order SUSY-QCD corrections to slepton pair production can be trivially obtained from the corresponding results for chargino/neutralino production. Numerically, the SUSY-QCD corrections for slepton production agree with the pure QCD corrections [11], provided the squark and gluino mass are not chosen smaller than the final state slepton mass.

in the form of the computer code PROSPINO [12].

Acknowledgements
We would like to thank P.M. Zerwas for his collaboration and encouragement. Moreover, we are grateful to R. Höpker and M. Klasen for their contribution to different parts of this work.

References

[1] M. Carena, R.L. Culbertson, S. Reno, H.J. Frisch and S. Mrenna, ANL-HEP-PR-97-98, hep-ph/9712022 and references therein.

[2] G.L. Kane and J.P. Leveillé, Phys. Lett. **B112** (1982) 227; P.R. Harrison and C.H. Llewellyn Smith, Nucl. Phys. **B213** (1983) 223 (Err. Nucl. Phys. **B223** (1983) 542); E. Reya and D.P. Roy, Phys. Rev. **D32** (1985) 645; S. Dawson, E. Eichten and C. Quigg, Phys. Rev. **D31** (1985) 1581; H. Baer and X. Tata, Phys. Lett. **B160** (1985) 159.

[3] W. Beenakker, R. Höpker, M. Spira and P.M. Zerwas, Phys. Rev. Lett. **74** (1995) 2905, Z. Phys. **C69** (1995) 163, and Nucl. Phys. **B492** (1995) 51.

[4] W. Beenakker, M. Krämer, T. Plehn, M. Spira and P.M. Zerwas, Nucl. Phys. **B515** (1998) 3.

[5] T. Plehn, Ph.D. Thesis, University Hamburg 1998, hep-ph/9809319; W. Beenakker, T. Plehn, M. Klasen, M. Krämer, M. Spira and P.M. Zerwas, in preparation.

[6] M. Carena, S. Mrenna and C.E.M. Wagner, ANL-HEP-PR-98-54, hep-ph/9808312; M. Spira, DESY-98-159, hep-ph/9810289, these proceedings.

[7] A. Denner, H. Eck, O. Hahn and J. Küblbeck, Nucl. Phys. **B387** (1992) 467.

[8] J. Collins, F. Wilczek and A. Zee, Phys. Rev. **D18** (1978) 242; W.J. Marciano, Phys. Rev. **D29** (1984) 580; R.K. Ellis, S. Dawson and P. Nason, Nucl. Phys. **B303** (1988) 607.

[9] S.P. Martin and M.T. Vaughn, Phys. Lett. **B318** (1993) 331; I. Jack and D.R.T. Jones, preprint LTH–400, hep-ph/9707278, to appear in 'Perspectives in Supersymmetry', ed. G. Kane, Singapore 1997.

[10] H.L. Lai et al., Phys. Rev. **D55** (1997) 1280.

[11] H. Baer, B.W. Harris and M.H. Reno, Phys. Rev. **D57** (1998) 5871.

[12] The computer code `PROSPINO` (see hep-ph/9611232) for the production of squarks, gluinos and stops at hadron colliders is available at http://wwwcn.cern.ch/~mspira/ or upon request from the authors. The next-to-leading order production cross sections for gaugino and slepton production will be included soon.

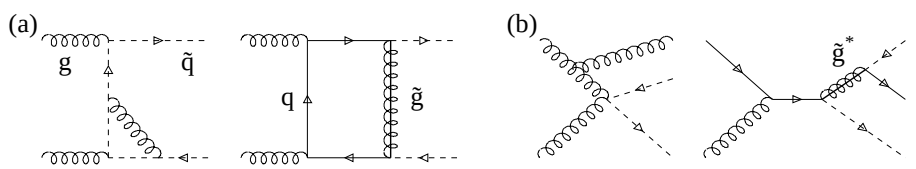

Figure 1: *Typical diagrams of the virtual (a) and real (b) corrections.*

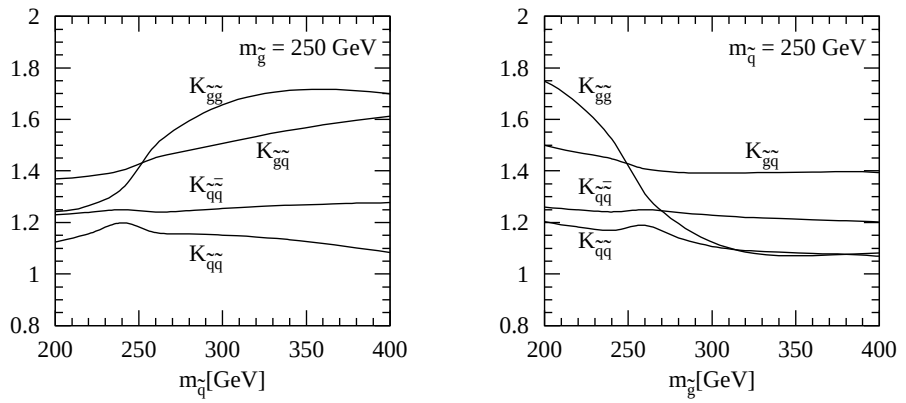

Figure 2: *K-factors of the squark and gluino production cross sections at* $Q = m$.

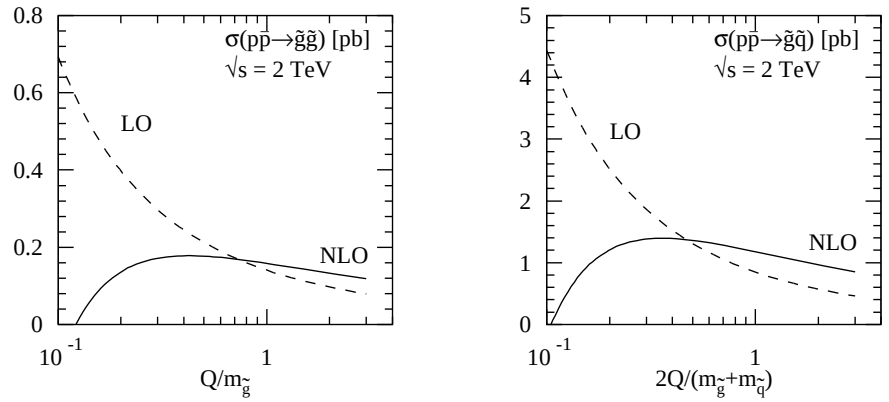

Figure 3: *Scale dependence of the total squark and gluino production cross sections for* $m_{\tilde{q}} = 250\ GeV$ *and* $m_{\tilde{g}} = 300\ GeV$.

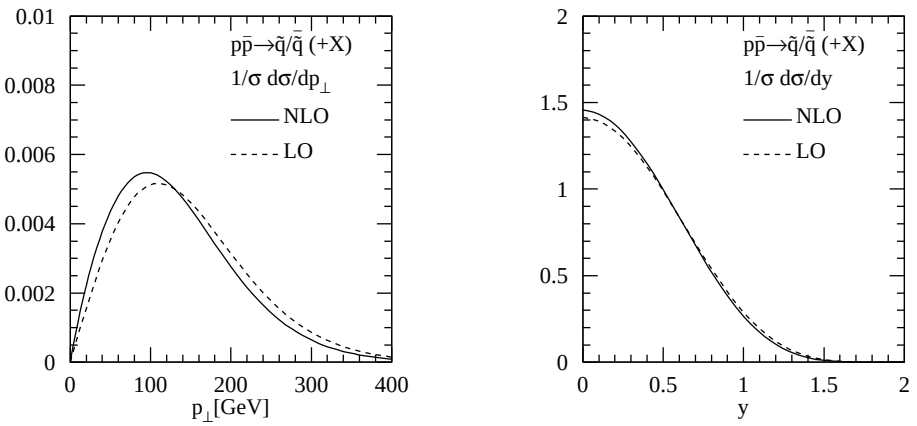

Figure 4: *Normalized transverse-momentum and rapidity distributions for squark production at* $Q = m$. *Mass parameters:* $m_{\tilde{q}} = 250\ GeV$ *and* $m_{\tilde{g}} = 300\ GeV$.

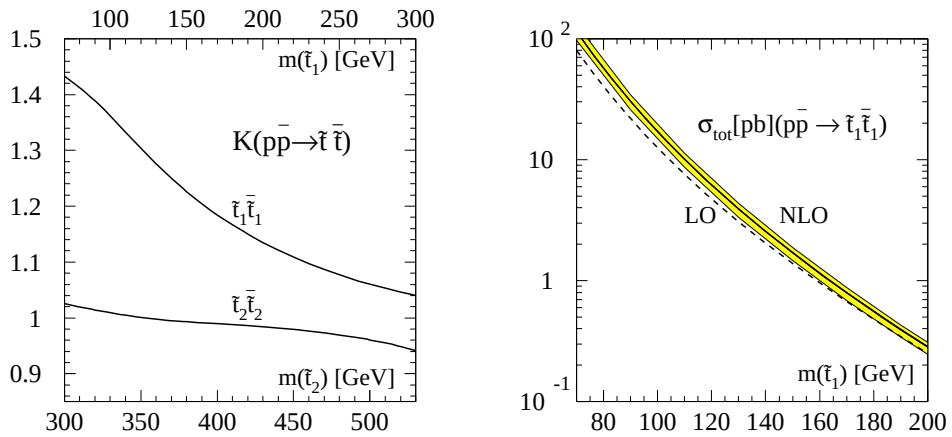

Figure 5: *Left: K-factor of the stop production cross sections at $Q = m_{\tilde{t}}$ as a function of the stop masses [top/bottom scale]. Right: Production cross sections for the light stop state. The thickness of the NLO curve represents the dependence of the cross sections on the stop mixing angle and the gluino and squark masses. The shaded band indicates the theoretical uncertainty due to the scale dependence [$m/2 < Q < 2m$].*

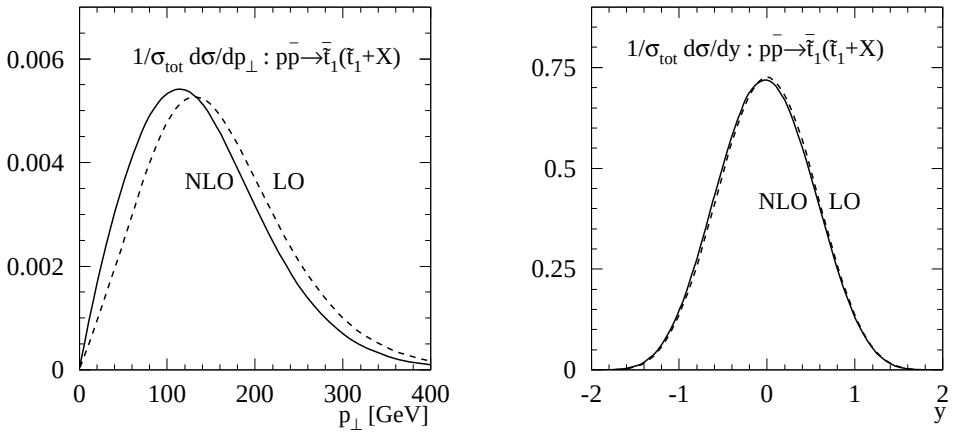

Figure 6: *Normalized transverse-momentum and rapidity distributions for stop production at $Q = m_{\tilde{t}} = 200\ GeV$.*

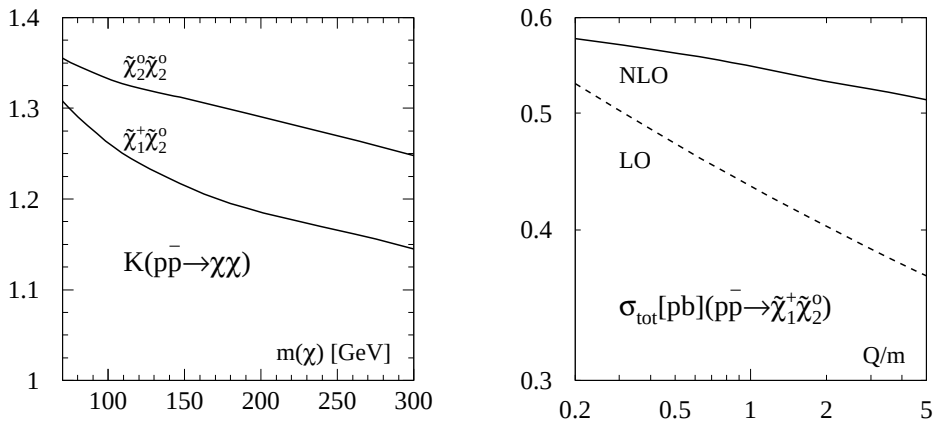

Figure 7: *Left: K-factor of the $\tilde{\chi}_2^0\tilde{\chi}_2^0$ and $\tilde{\chi}_1^+\tilde{\chi}_2^0$ production cross sections at the central scale $Q = m$. Right: Scale dependence of the $\tilde{\chi}_1^+\tilde{\chi}_2^0$ cross section. SUGRA parameters: $m_0 = 100\ GeV$, $A_0 = 300\ GeV$, $\tan\beta = 4$, $\mu > 0$.*

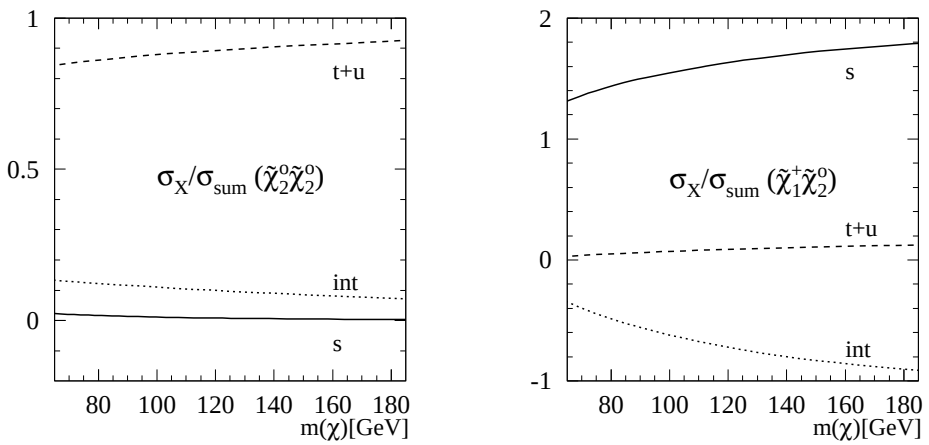

Figure 8: *The s-channel, $(t + u)$-channel and interference contributions to the leading order $\tilde{\chi}_2^0\tilde{\chi}_2^0$ and $\tilde{\chi}_1^+\tilde{\chi}_2^0$ production cross section. SUGRA parameters as in Fig. 7*

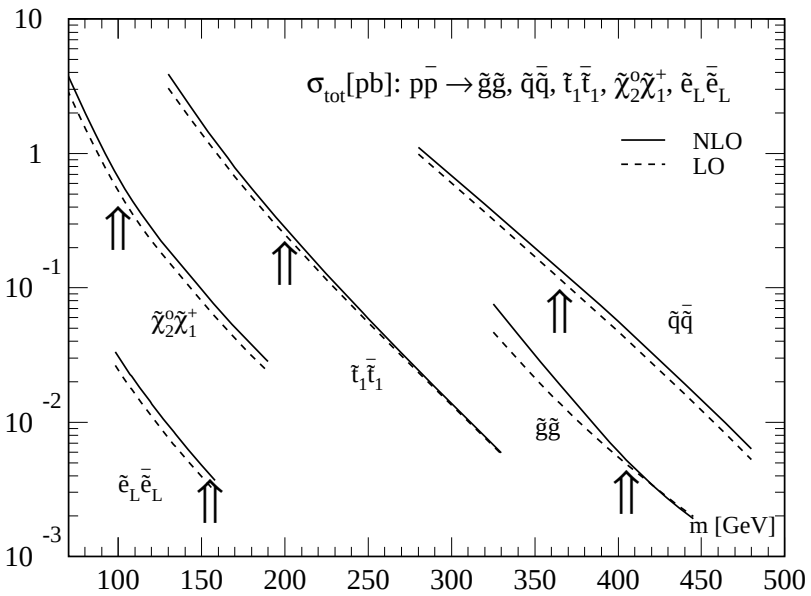

Figure 9: *The NLO production cross sections included in* `PROSPINO` *as a function of the final state particle mass; the arrows indicate the SUGRA inspired scenario:* $m_{1/2} = 150\ GeV$, $m_0 = 100\ GeV$, $A_0 = 300\ GeV$, $\tan\beta = 4$, $\mu > 0$. *All cross sections are given at the average mass scale of the massive final-state particles.*